JOURNAL OF AGRICULTURAL AND FOOD CHEMISTRY

In Vitro Actions on Human Cancer Cells and the Liquid Chromatography−Mass Spectrometry/Mass Spectrometry Fingerprint of Phytochemicals in Rice Protein Isolate

SHANGGONG YU,[†] NIANBAI FANG,[†,‡] QINGLIN LI,[†,‡] JIANXIANG ZHANG,[†,‡] HONGFENG LUO,[†,‡] MARTIN RONIS,[†,§] AND THOMAS M. BADGER*[,†,||]

Departments of Pharmaceutical Sciences, Pharmacology/Toxicology, and Physiology/Biophysics and Arkansas Children's Nutrition Center, University of Arkansas for Medical Sciences, 1120 Marshall Street, Little Rock, Arkansas 72202

Rice protein isolate (RPI) has been reported to reduce the incidence of 7,12-dimethylbenz[*a*]-anthracene-induced mammary tumors in rats. To determine the potential role of phytochemicals associated with the RPI, we studied in vitro antitumor activities of an ether fraction from RPI using human tumor cell lines, including two human breast carcinoma cell lines (MDA-MB-453 and MCF-7) and two myeloma cell lines (RPMI-8226 and IM-9). Concentration-dependent antiproliferative effects of the ether fraction were observed in all cell lines using the standard 3-[4,5-dimethylthiazol-2-yl]-2,5-diphenyltetrazolium bromide assay. Fraction-induced apoptosis ($P < 0.05$) was detected in all cell lines, and this was associated with the induction of proapoptotic bax protein and cdk inhibitors (p21) and the suppression of cdk4 and cyclin D1 activity. Liquid chromatography−mass spectrometry/mass spectrometry (LC-MS/MS) with both positive and negative modes was used to analyze the phytochemicals in the ether fraction from RPI. Fifty-seven phytochemicals were identified or characterized by their diagnostic fragmentation patterns and direct comparison with the authentic standards on the basis of electrospray ionization-MS/MS data. The major components bound to RPI were lysoglycerophospholipids, fatty acids, and fatty acid 3-[2-(2,3-dihydroxy-propoxycarbonyl)-2-hydroxy-ethoxy]-2-hydroxy-propyl esters.

KEYWORDS: Rice protein isolate (RPI); phytochemicals; anticancer properties; apoptosis; LC-MS/MS

INTRODUCTION

Diet is believed to be one of the most important lifestyle factors responsible for the lower incidence of breast and colon cancer in certain Asian countries as compared with the United States. Traditionally, Asians have consumed more soy, rice, and fish and less red meat and fat than Americans. In countries such as Japan, where the diet has become progressively more Westernized in recent years, the incidence of colon cancer has increased (*1*). Although soy foods have received considerable attention for their potential cancer protective effects (*2*−*8*), rice is a major staple of Asian diets that is generally consumed in greater quantities than soy. Rice possesses special dietary importance in Asia and is becoming increasingly recognized as providing health benefits in the areas of cancer (*9*−*18*), inflammation (*19*), and reductions in serum cholesterol (*20*−*23*). The majority of the studies in rice have focused on the phytochemicals of rice bran and colored rice. Much less attention has been given to the health effects of rice protein isolate (RPI) and the phytochemicals bound to RPI. RPI is in widespread use in the food industry and has been reported to lower cholesterol (*24*), to have antiatherogenic properties (*25*), and to block experimentally induced mammary tumorigenesis (*26*).

Our laboratory has previously demonstrated that rats fed AIN-93G diets made with RPI have a significantly lower incidence in 7,12-dimethylbenz[*a*]anthracene (DMBA)-induced mammary tumors (*27*), and we were interested in the potential mechanisms of this effect. The aim of the current study was to determine the potential antitumor-promoting effects of a phytochemical extract of RPI using in vitro bioassays. Furthermore, the phytochemicals bound to RPI were identified or characterized by their diagnostic fragmentation patterns and direct comparison with the authentic standards on the basis of electrospray ionization−mass spectrometry (ESI-MS)/MS data.

MATERIALS AND METHODS

Materials and Reagents. RPI was a gift from Riceland Foods, Inc. (Stuttgart, AR). RPI was produced using a proprietary process similar to that previously published (*28*) and employed amylase to hydrolyze the starch to syrup. The syrup was washed away in consecutive water washes, leaving the protein to be dried. Tissue culture media, fetal

* To whom correspondence should be addressed. Tel: 501-364-2875. Fax: 501-364-2818. E-mail: BadgerThomasm@uams.edu.
[†] Arkansas Children's Nutrition Center.
[‡] Department of Pharmaceutical Sciences.
[§] Department of Pharmacology/Toxicology.
[||] Department of Physiology/Biophysics.

10.1021/jf0605852 CCC: $33.50
Published on Web 05/23/2006

bovine serum, and trypan blue were purchased from Gibco (Grand Island, NY). Dimethyl sulfoxide (DMSO), 3-[4,5-dimethylthiazol-2-yl]-2,5-diphenyltetrazolium bromide (MTT), and propidium iodide were purchased from Sigma (St. Louis, MO). Annexin V−fluorescein isothiocyanate (Annexin V-FITC) was purchased from BD Bioscences (Palo Alto, CA). Lysis buffer was from Cell Signaling (Beverly, MA). Bio-Rad protein standard solution, Kaleidoscope Prestained Standards, and Immun-Blot PVDF Membrane for Protein Blotting (0.2 μm) were from Bio-Rad Laboratories (Hercules, CA). The primary antibodies against cdk4, $p21^{WAF1}$, Bax, and two secondary antibodies (anti-rabbit IgG antibody and anti-mouse IgG antibody) were purchased from Santa-Cruz Biotechnology (Santa Cruz, CA; catalog nos. 260, 397, 526, 2004, and 2005, respectively), and anti-cyclin D1 antibody was from Cell Signaling Technology (catalog #2926). Three standard mixtures including L-α-lysophosphatidylethanolamine (lyso-PE) (prepared from egg yolk, contains primarily stearic and palmitic acids), L-α-lysophosphatidylcholine (lyso-PC) [prepared by the action of phospholipase A on soybean L-α-phosphatidylcholine, contains primarily C-18 unsaturated fatty acids (FAs)], and L-α-lysophosphatidylinositol (prepared by the action of phospholipase A on soybean L-α-phosphatidylinositol, contains primarily palmitic and stearic acids), and FAs including linolenic acid, myristic acid, palmitoleic acid, linoleic acid, palmitic acid, oleic acid, and stearic acid were purchased from Sigma-Aldrich Chemical Co.

Preparation of the Ether Fraction from RPI. RPI (200 g) was extracted with 300 mL of 80% aqueous methanol at 5 °C for 24 h with occasional stirring. The slurry was filtered through a Büchner funnel with #4 Whatman filter paper. The extraction process was repeated with 80% (300 mL) aqueous methanol and followed with 50% methanol (300 mL × 2). The four extracts were combined and concentrated on a rotary evaporator under reduced pressure at room temperature until the methanol was removed. The aqueous extract (200 mL) was partitioned with ether (200 mL × 3). The combined ether phase was filtered through a Büchner funnel with #4 Whatman filter paper. The clear ether phase was evaporated under reduced pressure at room temperature followed by drying in a freeze dryer. The ether fraction (4.057 g) represented 2.03% of RPI.

Cell Cultures and Treatment. Four cell lines including two human breast carcinoma cell lines, estrogen receptor (ER)-negative MDA-MB-453 and ER positive MCF-7, and two myeloma cell lines, Epstein−Barr virus (EBV)-negative RPMI-8226 and EBV-positive IM-9, were obtained from the American Type Culture Collection (Rockville, MD). MDA-MB-453 and MCF-7 cells were maintained in Dulbecco's modified Eagle medium containing 0.37% $NaHCO_3$, 0.1% penicillin/streptomycin, and 10% fetal bovine serum. Two myeloma cell lines were maintained in RPMI-1640 supplemented with 10% fetal bovine serum, 100 U/L penicillin, 100 mg/L streptomycin, and 4 mmol L-glutamine. Cell cultures were incubated at 37 °C in a humidified atmosphere of 5% CO_2/95% air. The test fraction was dissolved in DMSO and mixture with medium before treatment. The final concentration of DMSO in treated cell medium was 0.1%. Two control groups were cells cultured in medium only (untreated) or in medium plus 0.1% DMSO.

Cell Proliferation Assay. Human breast cell lines (1×10^4/100 μL/well) were seeded in 96 well microplates and maintained for 48 h in the medium prior to treatment with different concentrations of an ether fraction from RPI. The MTT assay was carried out following previously described protocols (*29*). Myeloma cell lines (5×10^4/100 μL/well) were cultured overnight in 96 well microplates in medium free of phenol red, followed by treatment with different concentrations of the fraction. The MTT assay was conducted based on the published procedures (*30*). At the desired time point of treatment (24, 48, or 72 h), the medium was replaced with 100 μL of fresh culture medium free of phenol red containing 10 μL of 12 mM MTT solution. After incubation with MTT at 37 °C for 4 h, 100 μL of sodium dodecyl sulfate (SDS)−HCL solution was added to each well and incubated at 37 °C overnight. The viable cells in the wells converted MTT into purple formazan, which was measured at 540 nm. For observation of antiproliferative effects on the cell images, MCF-7 cells were seeded in six well microplates and treated with the fraction for 24 h. Antiproliferative effects on morphological changes of MCF-7 cells were captured at 200× magnification using the Spot program, Version 4.0 (Diagnostic Instruments, Inc., Sterling Heights, MI). All experiments were repeated at least three times using triplicate determinations.

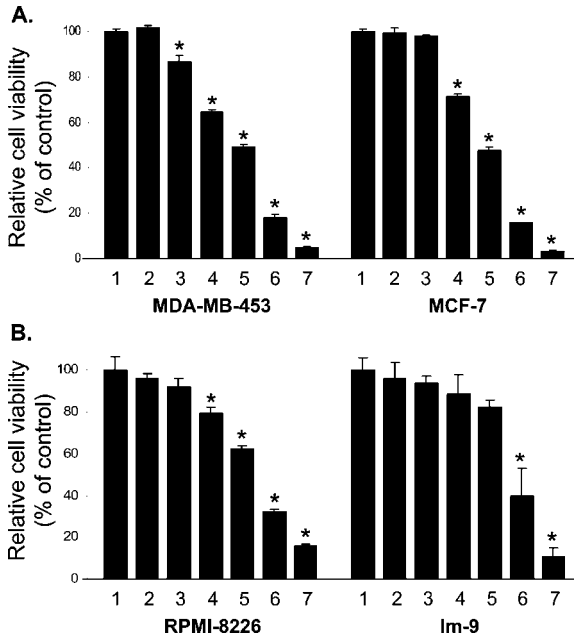

Figure 1. Antiproliferative effects of five concentrations of an ether fraction from RPI 24 h after treatment on (**A**) two human breast carcinoma cells (MDA-MB-453 and MCF-7) and (**B**) two myeloma cell lines (RPMI-8226 and IM-9) as determined by MTT assay. Key: 1, medium as control; 2, 0.1% DMSO; 3, 50 mg/L; 4, 100 mg/L; 5, 200 mg/L; 6, 400 mg/L; and 7, 800 mg/L. Each value represents the mean ± SD of three replicates; * = $P < 0.05$ vs control.

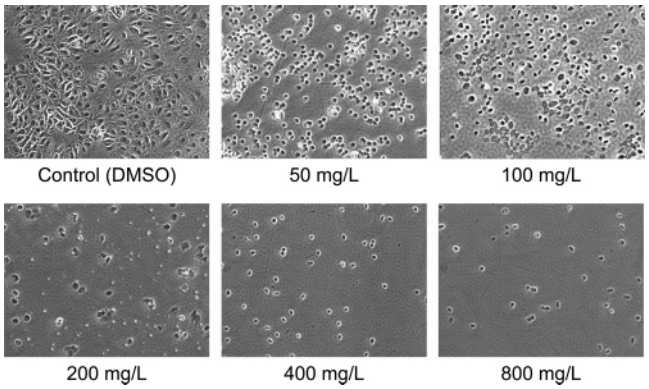

Figure 2. Antiproliferative effects on morphological changes of MCF-7 cells 24 h after treatments of different concentrations of the ether fraction from RPI.

Apoptosis Assays. The apoptotic effect of the ether fraction from RPI was determined by staining cells with Annexin V-FITC and PI (*31*). Cells were cultured in medium containing various concentrations of the fraction. The treated cells were harvested 24 h after treatment with the fraction and washed in ice-cold phosphate-buffered saline (PBS) and resuspended in 350 μL of Annexin V-binding buffer on ice. Five microliters of Annexin V-FITC was added to the cells and incubated on ice for 30 min in the dark. The cells were washed with PBS and resuspended in 350 μL of binding buffer on ice, and 4.5 μL of PI was added. After incubation in the dark for 10 min, the cells were analyzed by flow cytometry. Data plots were generated from analysis of ungated data, and representative dot plots indicate apoptotic tumor cells determined by PI and Annexin V-FITC staining. Viable cells (PI^-/Annexin V^-), newly apoptotic cells (PI^-/Annexin V^+), and already apoptotic cells (PI^+/Annexin V^+) are located in the lower left (LL), lower right (LR), and upper right (UR) quadrants of data plots, respectively. The total apoptotic cells represented the sum of PI^-/

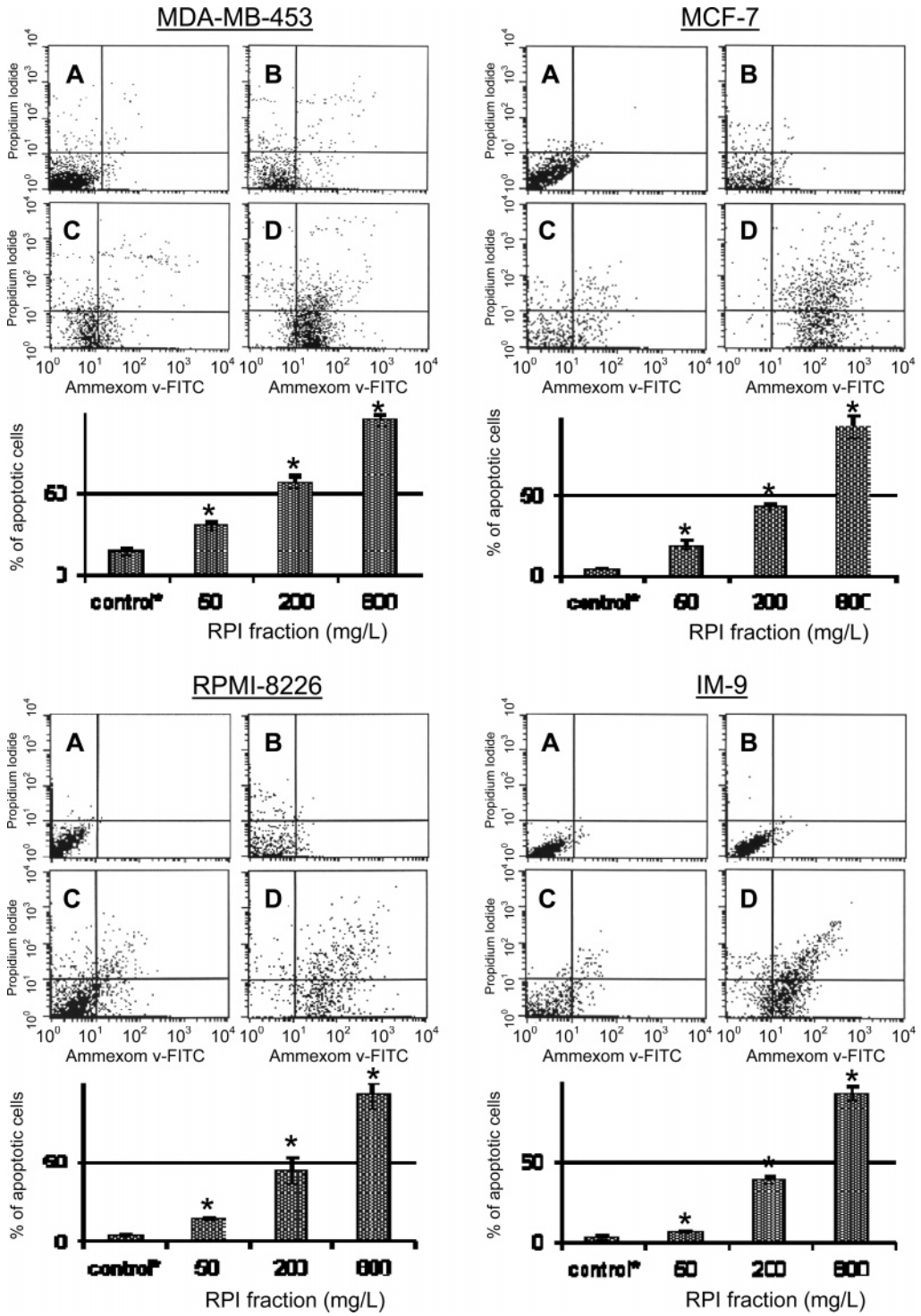

Figure 3. Ether fraction-induced apoptosis in two human breast carcinoma cell lines and two myeloma cell lines 24 h after treatment. Representative dot plots showing apoptotic tumor cells determined by PI and Annexin V-FITC staining. Alive cells (PI^-/Annexin V^-), newly apoptotic cells (PI^-/Annexin V^+), and already apoptotic cells (PI^+/Annexin V^+) are located at LL, LR, and UR, respectively. (**A**) Control (0.1% DMSO), (**B**) 50 mg/L, (**C**) 200 mg/L, and (**D**) 800 mg/L. The percentages of apoptotic cells are the sum of PI^-/Annexin V^+ (newly apoptotic cells) and PI^+/Annexin V^+ (already apoptotic) cells population by flow cytometry analysis; * = $P < 0.05$ vs control.

Annexin V^+ (newly apoptotic) and PI^+/Annexin V^+ (already apoptotic) cell populations (*31*).

Western Blot Analysis. MDA-MB-453 and MCF-7 cells were incubated in 75 cm^2 flasks. The cells were treated with an ether fraction from RPI at 50, 200, or 800 mg/L when the cell density reached 80−90% confluence. The cells were washed with cold PBS twice after 24 h, harvested in cell lysis buffer containing 1 mM phenylmethylsulfonyl fluoride with sonication while in an ice bath, and microcentrifuged. The protein concentration in the cell lysate was measured using Bio-Rad protein standard solution. Equal amounts of total protein were mixed with 5× loading buffer (25% glycerol, 7.5% SDS, 5% 2-mercaptoethanol, 0.05% bromophenol blue, and 156 mM Tris-HCL, pH 6.8) and fractionated by electrophoresis on 15% SDS−polyacrylamide gel electrophoresis (PAGE). Kaleidoscope Prestained Standards were used as molecular weight markers. Proteins were electrotransferred to immune-blot PVDF membranes using transfer buffer. After blocking with 5% w/v nonfat dry milk in TBS overnight at 4 °C, the membranes were incubated for 2 h at room temperature with appropriate dilutions

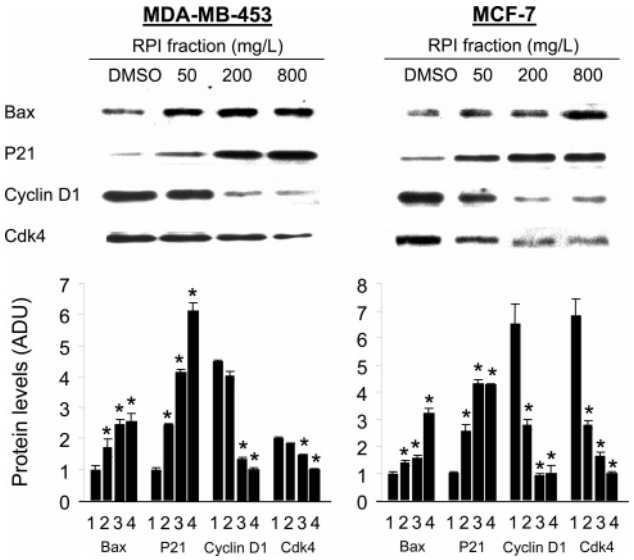

Figure 4. Expression of bax, p21, cyclin D1, and cdk4 in MDA-MB-453 and MCF-7 cells with Western blot analysis. Cells were treated with the ether fraction from RPI in various doses for 24 h. Key: 1, 0.1% DMSO as control; 2, 50 mg/L; 3, 200 mg/L; and 4, 800 mg/L. Each value represents the mean ± SD of three replicates; * = $P < 0.05$ vs control.

of primary antibodies in blocking buffer, anti-cdk4 (1:600), anti-p21^{WAF1} (1:500), anti-Bax (1:600), and anti-cyclin D1 (1:2000), and washed three times with TBS containing 0.1% Tween 20. Subsequently, the membranes were incubated with the peroxidase-conjugated anti-rabbit secondary antibody diluted in blocking buffer, 1:6000 for anti-cdk4, 1:5000 for anti-p21^{WAF1}, and anti-Bax, or the peroxidase-conjugated anti-mouse secondary antibody 1:3000 for anti-cyclin D1. Antibody-bound proteins were visualized by ECL plus Western blotting analysis system (Amersham Pharmacia Biotech, United Kingdom).

LC-MS/MS Analysis. The ether fraction from RPI was directly analyzed by LC-MS/MS using a Bruker model Esquire-LC multiple ion trap mass spectrometer equipped with an Agilent 1100 series liquid chromatograph and HP ChemStation for data collection and manipulation. A 150 mm × 4.6 mm i.d Eclipse XDB-C8 column (Agilent Technologies, Wilmington, DE) was used with LC solvent at a flow rate of 0.8 mL/min. The LC gradient was acetonitrile (solvent B) in H_2O (solvent A). The constituents in the eluant were monitored by MS and a diode array detector set at five wavelengths of 200 ± 10, 240 ± 10, 290 ± 10, 320 ± 10, and 355 ± 10 nm. MS with both positive and negative modes was used to characterize or identify a wide range of natural products. For optimum MS analysis, 10 mmol/L ammonium acetate (for negative-ion mode) or 2% formic acid (for positive-ion mode) in methanol was used as an ionization reagent and added at a flow rate of 0.2 mL/min via a tee in the eluant stream of the high-performance liquid chromatograph (HPLC) just prior to the mass spectrometer. Conditions for ESI-MS in both negative- and positive-ion mode included a capillary voltage of 3200 V, a nebulizing pressure of 33.4 psi, a drying gas flow of 8 mL/min, and at 250 ° C. Parameters that control the atmospheric pressure interface (API) and the mass spectrometer were set via the Smart Tune with a compound stability of 50% and a trap drive level of 50%. Ion charge control (ICC) was on including the following: target, 5000; maximum accumulation time, 50.00 ms; scan, *m*/*z* 80.00−850.00; averages, 10; and rolling averaging, off. Conditions for automatic MS/MS were as follows: width of the isolation, 4.0; fragmentation amplitude, 1.00 V; and number of parents, 1.

Statistical Analyses. Results are expressed as means ± standard deviations (SD) for at least three replicate determinations for each assay. The data shown in **Figures 2**, **4**, and **5** were analyzed by one-way analysis of variance and Dunnett's posthoc test to compare treatments vs the control using SigmaStat software. P values < 0.05 were considered statistically significant.

RESULTS AND DISCUSSION

We have previously studied the effects of SPI on mammary gland development and DMBA-induced mammary tumors and found a consistently lower incidence of tumors, increased latency, and lower multiplicity (*32*). Morita et al. (*26*) found a lower incidence of the DMBA-induced mammary gland tumors in rats fed diets made with RPI when compared with rats fed diets made with either casein or SPI (*26*). Similar results have been reported in our laboratory (*27*). These results are of potential importance because while Westernized populations do not consume high levels of either rice or soy, there is far more rice consumed in countries such as the United States than soy foods, and if a health advantage could be established, there is

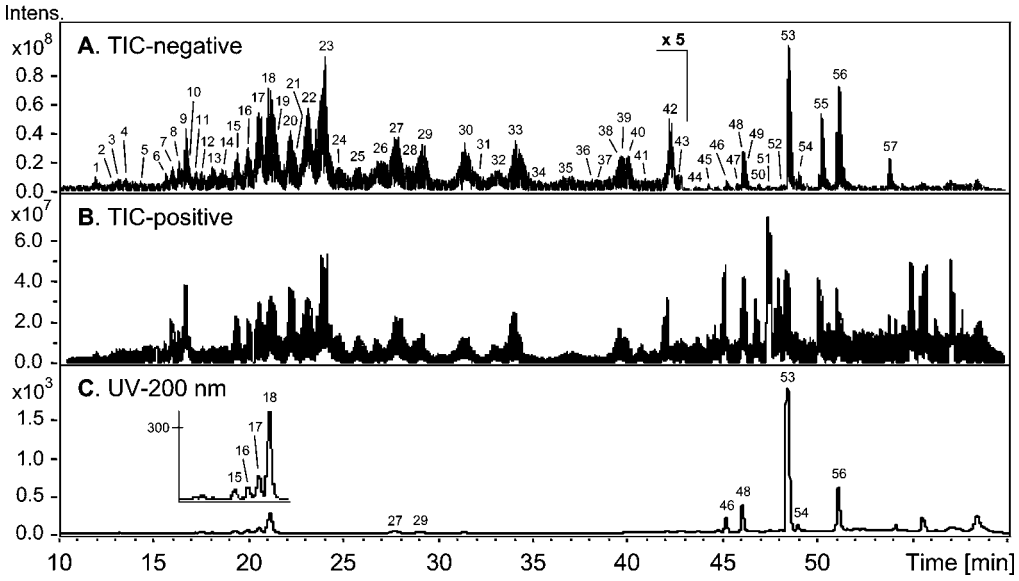

Figure 5. LC/MS/MS fingerprints of an RPI ether fraction: (**A**) negative TIC, (**B**) positive TIC, and (**C**) UV (200 ± 10 nm) chromatogram. Lyso-PC: **7**, **9**, **10**, **12**, **16**, **18**, **20**, **23**, **25**, **27**, **35**, and **38** (**Figure 6A**); lyso-PE: **3**, **4**, **6**, **8**, **11**, **15**, **17**, **19**, **22**, **24**, **26**, **34**, **36**, and **41** (**Figure 6B**); lyso-PG: **37**, **39**, and **43** (**Figure 6C**); FAs: **1**, **2**, **5**, **13**, **14**, **21**, **30**, **32**, **42**, **45**–**51**, and **53**–**57** (**Table 1**); and FA DPHEHP esters: **28**, **29**, **31**, **33**, **40**, **44**, and **52** (**Table 2**).

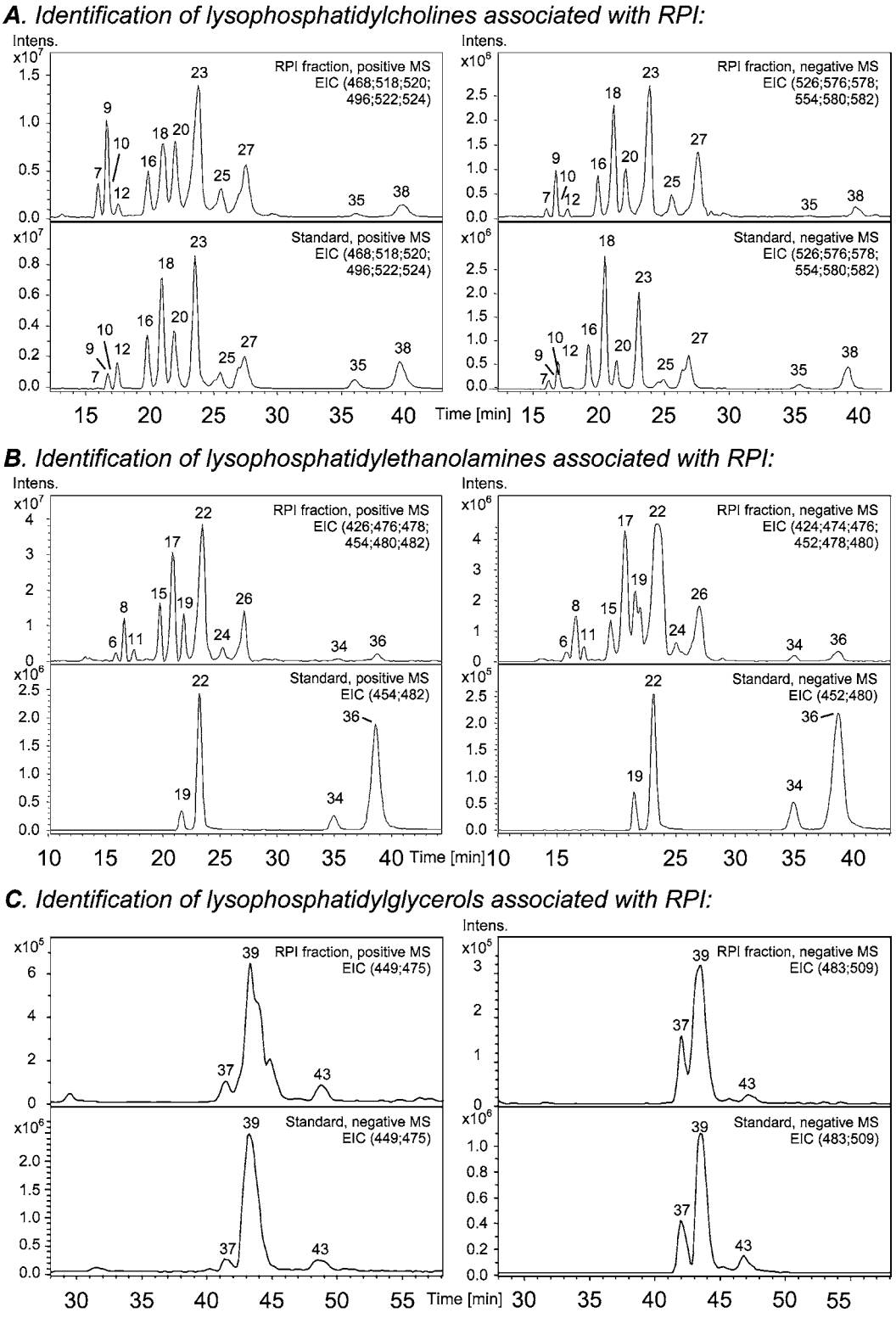

Figure 6. LC-MS chromatograms of lyso-PL in the ether fraction and lyso-PL standards. Lyso-PC: **7**, lyso/14:0a-PC; **9**, 14:0a/lyso-PC; **10**, lyso/18:3a-PC; **12**, 18:3a/lyso-PC; **16**, lyso/18:2a-PC; **18**, 18:2a/lyso-PC; **20**, lyso/16:0a-PC; **23**, 16:0a/lyso-PC; **25**, lyso/18:1a-PC; **27**, 18:1a/lyso-PC; **35**, lyso/18:0a-PC; and **38**, 18:0a/lyso-PC. Lyso-PE: **3**,* OH-lyso/18:2a-PE; **4**,* OH-18:2a/lyso-PE; **6**, lyso/14:0a-PE; **8**, 14:0a/lyso-PE; **11**, 18:3a/lyso-PE; **15**, lyso/18:2a-PE; **17**, 18:2a/lyso-PE; **19**, lyso/16:0a-PE; **22**, 16:0a/lyso-PE; **24**, lyso/18:1a-PE; **26**, 18:1a/lyso-PE; **34**, lyso/18:0a-PE; **36**, 18:0a/lyso-PE; and **41**, 20:1a/lyso-PE. Lyso-PG: **37**, lyso/16:0a-PG; **9**, 16:0a/lyso-PG; and **43**, lyso/18:1a-PG. *Compounds **3** and **4** are trace components in RPI, and LC/MS/MS data are available as Supporting Information.

a greater likelihood that Westerners would incorporate more rice into their diets than soy. In the current report, the phytochemicals in the ether fraction were obtained from a partition between ether and aqueous methanol extract of RPI. The ether fraction (4.057 g from 200 g of RPI) represented 2.03% of RPI. To determine the potential role of phytochemicals associated with the RPI, we studied in vitro antitumor activities of an ether fraction using human tumor cell lines and determined the identity of phytochemicals in the ether fraction from the RPI.

Table 1. ESI-MS/MS Data for Free FAs Associated with RPI

no. in Figure 1	R_t (min)	ionization mode	product ions from CID, *m/z* (relative intensity %) parent ion	[P – H_2O][a]	other ions	structure
			FAs with Two Oxygen Atoms (Nonhydroxy FAs)			
46	45.0	negative	279 $[M-H]^-$	261 (100)		18:2
		positive	263 $[M+H-H_2O]^+$	245 (100)	165 (36), 149 (51), 121 (48), 93 (57)	
47	45.6	negative	255 $[M-H]^-$	237 (100)		16:0
48[b]	45.9	negative	277 $[M-H]^-$	259 (32)	233 (100)	18:3 (linolenic acid)
		positive	279 $[M+H]^+$	261 (26)	191 (73), 173 (100), 151 (53), 131 (49)	
49[b]	46.1	negative	227 $[M-H]^-$	209 (100)		14:0 (myristic acid)
50	46.7	negative	255 $[M-H]^-$	237 (100)		16:0
51[b]	47.2	negative	253 $[M-1]^-$	235 (100)		16:1 (palmitoleic acid)
53[b]	48.2	negative	279 $[M-1]^-$	261 (100)		18:2 (linoleic acid)
		positive	263 $[M+H-H_2O]^+$	245 (100)	217 (43), 189 (69), 163 (55), 105 (29)	
54	48.8	negative	279 $[M-1]^-$	261 (100)		18:2
		positive	263 $[M+H-H_2O]^+$	245 (100)	189 (50), 161 (33), 127 (23), 109 (25)	
55[b]	50.0	negative	255 $[M-1]^-$	237 (100)		16:0 (palmitic acid)
		positive	257 $[M+H]^+$	239 (70)	187 (50), 145 (100), 117 (72), 103 (69)	
56[b]	50.8	negative	281 $[M-1]^-$	263 (100)		18:1 (oleic acid)
		positive	265 $[M+H-H_2O]^+$	247 (100)	191 (36), 151 (74), 111 (65), 95 (72)	
57[b]	53.7	negative	283 $[M-1]^-$	265 (100)		18:0 (stearic acid)
		positive	285 $[M+H]^+$	267 (39)	201 (94), 191 (71), 159 (100), 145 (58)	
			FAs with Three Oxygen Atoms (Monohydroxy FAs)			
30	31.2	negative	295 $[M-H]^-$	277 (100)	233 (17), 195 (51), 179 (7), 171 (22)	OH-18:2
		positive	279 $[M+H-H_2O]^+$		261 (23), 243 (71), 159 (59), 123 (100)	
32	33.0	negative	295 $[M-H]^-$	277 (69)	233 (6), 251 (3), 171 (100), 123 (14)	OH-18:2
		positive	279 $[M+H-H_2O]^+$	261 (23)	243 (100), 192 (45), 179 (71), 121 (47)	
42	41.9	negative	295 $[M-H]^-$	277 (100)	233 (4), 171 (77), 141 (2), 125 (3)	OH-18:2
		positive	279 $[M+H-H_2O]^+$	261 (64)	224 (38), 179 (46), 153 (44), 124 (100)	
45	44.2	negative	297 $[M-H]^-$	279 (63)	197 (3), 171 (100), 155 (15)	OH-18:1
			FAs with Four Oxygen Atoms (Hydroxylated and/or Hydroperoxidated FAs)			
5	14.2	negative	311 $[M-H]^-$	293 (100)	275 (11), 231 (21), 181 (12), 157 (69)	diOH-18:2
13	18.0	negative	313 $[M-H]^-$	295 (100)	277 (20), 195 (21), 183 (90)	diOH-18:1
		positive	337 $[M+Na]^+$		263 (46), 245 (54), 207 (53), 176 (100)	
14	18.6	negative	313 $[M-H]^-$	295 (33)	277 (34), 201 (100), 171 (45), 165 (25)	diOH-18:1
		positive	337 $[M+Na]^+$		261 (72), 243 (87), 226 (100), 188 (72)	
21	22.4	negative	315 $[M-H]^-$	297 (100)	279 (15), 171 (39), 155 (9), 141 (7)	diOH-18:0
			FAs with Five Oxygen Atoms (Hydroxylated and/or Hydroperoxidated FAs)			
1	11.9	negative	329 $[M-H]^-$	311 (42)	293 (63), 229 (100), 211 (51), 171 (55)	triOH-18:1
		positive	353 $[M+Na]^+$	335 (100)		
2	12.8	negative	329 $[M-H]^-$	311 (32)	293 (17), 211 (40), 195 (100)	triOH-18:1
		positive	353 $[M+Na]^+$	335 (72)	321 (85), 289 (81), 235 (100), 191 (98)	

[a] Ions [P – H_2O] are the ion [parent – H_2O]$^+$ for positive ionization mode MS and the ion [parent – H_2O]$^-$ for negative ionization mode MS. [b] Compounds were identified by direct comparison in LC-MS/MS analysis.

Antiproliferative Properties of the Ether Fraction from RPI. The MTT assay was used to assess antiproliferative effects of the ether-soluble phytochemicals from RPI in four human cancer cell lines. Following incubation with different concentrations of the fraction (0, 50, 100, 200, 400, and 800 μg/mL) for 24 h, there was a concentration-dependent reduction of cell viability (**Figure 1**). IC_{50} values for two human breast carcinoma cells (MDA-MB-453 and MCF-7) and two myeloma cell lines (RPMI-8226 and IM-9) were 194.14 ± 8.07, 188.56 ± 6.56, 271.19 ± 17.89, and 353.21 ± 54.18 mg/L, respectively. It is important to note that different protocols were used for the MTT bioassay of myeloma cells (growth properties, suspension) and breast cells (growth properties, adherent); thus, IC_{50} values of myeloma cells should not be used to compare with that of breast cells for their potency. Similar fraction potencies (IC_{50} used as an indicator of their potency) in the MTT assays were observed at 48 and 72 h treatments of the fraction in all cell lines (data not shown). MCF-7 cells seeded in six well microplates were treated with the fraction for 24 h, and the morphological changes of cells were captured at 200× magnification using the Spot program, version 4.0. Clear antiproliferative effects were observed at 50 mg/L of the extract (**Figure 2**), while no antiproliferative effects were observed at the same concentration in the MTT bioassay (**Figure 1**).

Ether Fraction-Induced Apoptosis. Fraction-induced apoptosis on MDA-MB-453, MCF-7, RPMI-8226, and IM-9 cells was evaluated at 0 (0.1% DMSO), 50, 200, and 800 mg/L of the fraction. The treated cells were sequentially stained with annexin V-FITC and propidium iodide following 24 h of treatment with the fraction. The staining pattern with annexin V-FITC or/and propidium iodide of the treated cells and their controls was quite different. Gradual dose-dependent decreases of viable cells and increases of apoptotic cells were observed in the human breast carcinoma and the myeloma lines (**Figure 3**). Approximately 200 mg/L of the fraction could induce apoptosis in 50% of the population. The results were consistent with the antiproliferative effect of the fraction.

Expression of Cdk4, Bax, Cyclin D1, and p21^{WAF1}. MDA-MB-453 and MCF-7 cells were used to elucidate the mechanisms of the fraction-induced apoptosis. The cells were treated with the fraction at 0 (0.1% DMSO), 100, 400, and 800 mg/L, and the treated cells were examined by Western blot analysis. As shown in **Figure 4**, the levels of bax and p21 protein were

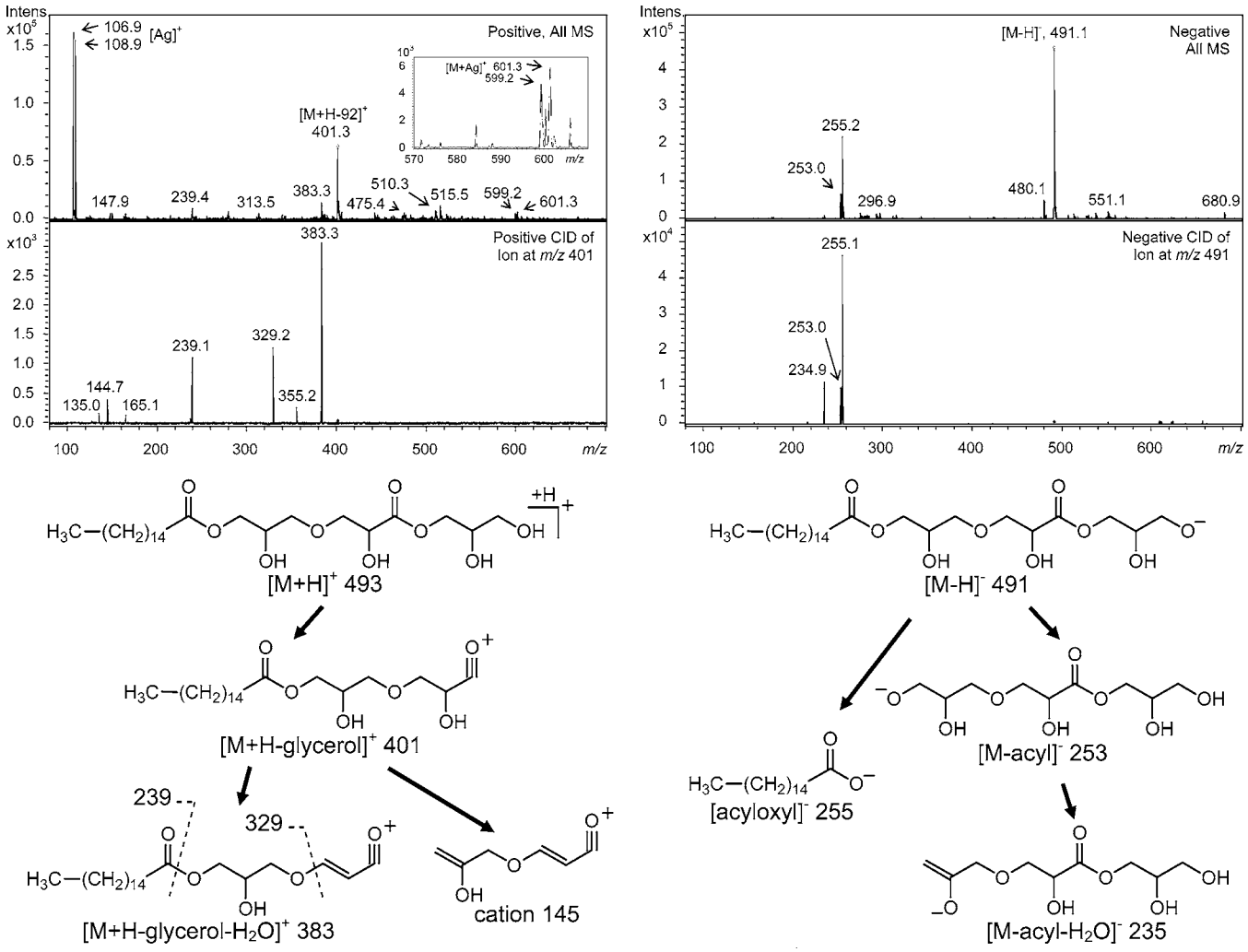

Figure 7. Mass spectra of compound **33** and proposed diagnostic fragmentation pathways for FA DPHEHP esters.

increased, and in contrast, the levels of cyclin D1 and Cdk4 were decreased 24 h after fraction treatment.

In these studies, the in vitro bioassay of an ether fraction of RPI in human breast cell lines indicated a dose-dependent decrease in the numbers of viable cells, increases in apoptotic cell numbers, and suppression of proliferation. The results suggest that the fraction-induced apoptosis may be mediated through increasing proapoptotic bax protein expression. MDA-MB-453 and MCF-7 cells treated with the fraction also showed up-regulation of p21 and down-regulation of cyclin D1 and cdk4. A central role is played by cdks in the cell cycle of mammalian cells (*33*), and progression through the cell cycle is accelerated by cyclins and cdks and decelerated by cdk inhibitors (such as p21). The D type cyclins (cyclins D1, D2, and D3) are involved in regulation of transition from G1 to S phases of the cell cycle. Also, it is reasonable to assume that the fraction may induce G1 arrest in cells via the induction of cdk inhibitors (p21), with the suppression of cyclin D1 and cdk4 activity. Furthermore, we studied myeloma cell lines to determine if these effects were limited to just mammary tumor cells or if these protective effects might be applicable to other cancers. Our results suggested that phytochemicals in RPI act similarly in myeloma cell lines. It should be noted that the concentrations of the fraction required to cause these effects were somewhat high, but it was a crude fraction and further fractionation is expected to reveal one or more phytochemicals with high potency.

LC-MS/MS Fingerprint of an Ether Fraction from RPI. The ether fraction was directly analyzed by LC-MS/MS. Five wavelengths set on the diode array detector and MS with positive and negative modes were used to monitor the phytochemicals in the eluant from LC. The major UV peaks were shown in the 200 nm chromatogram (**Figure 5C**) and identified as unsaturated FAs by comparison with corresponding standards. The negative total ion chromatograms (TIC) (**Figure 5A**) and UV (200 nm) profiles, combined with a lack of significant peaks detected at 240, 290, 320, and 355 nm, suggested that major phytochemicals in an ether fraction from RPI were common FAs (compounds **48**, **53**, and **55**−**57**). However, the positive TIC profile shown in **Figure 5B** revealed a much more complicated composition for phytochemicals associated with RPI.

Identification of Lysophospholipids (Lyso-PL). Twelve lyso-PCs, 14 lyso-PEs, and three lysophosphatidylglycerols (lyso-PG) were identified by direct comparison with their corresponding standards in LC-MS (**Figure 6**) and their unique fragments and neutral losses in the ESI-MS with both positive- and negative-ion modes (*34*). The MS data for lyso-PC, lyso-PE, and lyso-PG for RPI are very similar to those previously published for soy protein isolate (*34*), except for one ion in the negative MS of lyso-PC. While lyso-PC yielded an abundance of negative molecular ion species $[M + OAc]^-$ in the neutral solvent system in this study, abundant $[M + HCOO]^-$ was generated in the formic acid solvent system instead (*34*). The

Table 2. ESI-MS Data for FA DPHEHP Esters Associated with RPI

		positive ionization mode, *m/z* (relative intensity %)												
		major peaks in MS						product ions CID of $[M + H - glycerol]^+$						
no. in **Figure 1**	R_t (min)	$[M + H]^+$	$[M + Na]^+$	$[M + NH_4]^+$	$[M + H - H_2O]^+$	$[M + H - glycerol]^+$	$[M + H - glycerol - H_2O]^+$	parent $[M + H - glycerol]^+$	$[parent - H_2O]^+$	$[acyl]^+$	$[acyloxy]^+$	$[parent - C_3H_4O_2]^+$	cation at *m/z* 145	other ions
28	28.3	493 (1)	515 (0)	510 (0)	475 (0)	401 (100)	383 (11)	401	383 (60)	239 (100)	257 (18)		145 (12)	335 (51)
29	29.0	517 (0)	539 (22)	534 (18)	499 (10)	425 (100)	407 (42)	425	407 (100)	263 (53)		353 (18)		389 (68), 283 (57)
31	31.9	493 (0)	515 (30)	510 (19)	475 (16)	401 (100)	383 (29)	401	383 (100)	239 (47)	257 (3)	329 (20)	145 (41)	341 (24), 127 (15)
33	33.9	493 (0)	515 (6)	510 (9)	475 (3)	401 (100)	383 (8)	401	383 (100)	239 (12)	257 (3)	329 (3)	145 (8)	163 (5), 127 (4)
40	39.9	519 (17)	541 (42)	536 (14)	501 (6)	427 (100)	409 (61)	427	409 (100)	265 (37)	283 (20)	355 (10)	145 (8)	391 (44), 373 (31)
44	43.4	521 (0)	543 (2)	538 (12)	503 (3)	429 (100)	411 (14)	429	411 (100)	267 (23)	285 (1)	357 (11)	145 (12)	393 (5), 351 (16)
52	47.6	549 (0)	571 (7)	564 (9)	531 (0)	457 (100)	439 (56)	457	439 (100)	295 (8)	313 (3)	385 (7)		421 (9), 293 (10)

		negative ionization mode, *m/z* (relative intensity %)							
		major peaks in MS			product ions CID of $[M - H]^-$				
no. in **Figure 1**	R_t (min)	$[M - H]^-$	$[acyloxy]^-$	$[M - H - acyl]^-$	parent $[M - H]^-$	$[acyloxy]^-$	$[M - H - acyl]^-$	$[M - H - acyloxy]^-$	proposed tentative structures
28	28.3	491 (100)	255 (75)	253 (39)	491	255 (100)	253 (10)	235 (20)	stereoisomer of compound **33** (**Figure 7**)
29	29.0	515 (100)	279 (44)	253 (11)	515	279 (100)	253 (8)	235 (3)	linoleic acid (18:2) FA DPHEHP esters
31	31.9	491 (100)	255 (58)	253 (12)	491	255 (100)	253 (20)	235 (30)	stereoisomer of compound **33** (**Figure 7**)
33	33.9	491 (100)	255 (48)	253 (15)	491	255 (100)	253 (21)	235 (25)	palmitic acid (16:0) DPHEHP esters (**Figure 7**)
40	39.9	517 (100)	281 (35)	253 (9)	517	281 (100)	253 (4)	235 (7)	oleic acid (18:1) DPHEHP esters
44	43.4	519 (100)	283 (36)	253 (12)	519	283 (100)	253 (3)	235 (7)	stearic acid (18:0) DPHEHP esters
52	47.6	547 (100)	311 (30)		547	311 (100)	253 (36)		arachidic acid (20:0) DPHEHP esters

MS data for lyso-PL are not shown and are available as Supporting Information.

Identification of FAs. Seven common FAs, linolenic acid (**48**), myristic acid (**49**), palmitoleic acid (**51**), linoleic acid (**53**), palmitic acid (**55**), oleic acid (**56**), and stearic acid (**57**), were identified by comparison with their corresponding standards in LC-MS/MS analyses. Also, 14 FAs were characterized by LC-MS/MS analysis including retention time and product ions from collision-induced dissociation (CID) (**Table 1**). FAs were much more sensitive to negative ionization than positive ionization because of the carboxyl group. Carboxylate anions $[M - H]^-$ were the major molecular ion species in the MS spectra, and CID of $[M - H]^-$ yielded abundant ions $[M - H - H_2O]^-$. For the positive ionization, ESI-MS behavior of FAs was complicated. All FAs with three oxygen atoms (monohydroxy FAs) yielded abundant positive ion species $[M + H - H_2O]^+$, and all FAs with four or five oxygen atoms (hydroxylated and/or hydroperoxidated FAs) had the tendency to form the ion species $[M + Na]^+$ instead (**Table 1**).

Identification of FA 3-[2-(2,3-Dihydroxy-propoxycarbonyl)-2-hydroxy-ethoxy]-2-hydroxy-propyl Esters (DPHEHP Esters). Compound **33**, in its negative ESI-MS, yielded an anion at *m/z* 491 as the most abundant ion, along with lesser abundant ions at *m/z* 255, 253, and 235 (**Figure 7**). These three ions were produced by the CID of anion at *m/z* 491. The anion at *m/z* 491 was designed as a deprotonated molecular ion $[M - H]^-$ in accord with the $C_{25}H_{48}O_9$ formula for **33**. However, protonated molecular ions $[M + H]^+$ at *m/z* 493 were not found in the positive MS spectrum of **33** (**Figure 7** and **Table 2**). Two positive molecular ion species, $[M + Na]^+$ at *m/z* 515 and $[M + NH_4]^+$ at *m/z* 510, appeared in the positive MS spectrum of **33**, but they were not abundant. To confirm 492 as the molecular weight of **33**, the addition of 50 μg/mL silver perchlorate post-HPLC was used in LC-MS/MS analysis. This method can be used to form the Ag^+−lipid adducts and enhance the ESI of neutral lipids (*35*). Furthermore, the naturally occurring isotopes of silver (^{107}Ag and ^{109}Ag) are of almost equal abundance, resulting in a very characteristic two mass doublet for the two Ag^+ adduct ions. In this study, the characteristic two Ag^+ adducts of compound **33** at *m/z* 599 (^{107}Ag-**33**) and 601 (^{109}Ag-**33**) were produced in the positive MS spectrum (**Figure 7**) and confirmed the $C_{25}H_{48}O_9$ formula for **33**. The structure of **33** was assigned as hexadecanoic acid DPHEHP ester based on product ions from CID of $[M - H]^-$ and $[M + H - glycerol]^+$ (**Figure 7**). The fragmentation patterns of compounds **28**, **29**, **31**, **40**, **44**, and **52** were identical to that of **33** (**Table 2**), which suggested that these compounds should be FA DPHEHP esters. Because neither NMR data of these minor compounds nor their standards were available, identification of these compounds could not be completed by LC-MS/MS and assigned structures in this study were tentative.

The chemical fingerprint of the ether fraction from RPI was established by LC-MS, which indicated that lyso-PLs, FAs, and FA DPHEHP esters are the major components. Lyso-PLs are normal constituents of cellular membranes (*36*, *37*), body fluids, and lipoproteins (*38*, *39*) and have been known for decades to

have diverse effects on growth and cellular functions in multiple organ systems implicated in pathophysiological conditions, including cardiovascular disease, cancer, neurological disease, and immune function (*40*−*42*). NF-kB activation has been associated with increased proliferation and decreased apoptosis at lower concentrations, but higher concentrations (50 mmol/L) of lysoPC inhibited endothelial NF-kB activity (*43*). Cytotoxic effects of lyso-PC in higher concentrations were observed in MCF-7 cells in our laboratory (data not shown). There are no published data on the effects of lyso-PLs resulting from dietary intake.

The major FA components in RPI were identified as the common FAs linolenic acid, linoleic acid, palmitic acid, oleic acid, and stearic acid. Also, 10 oxygenated FAs (hydroxylated and/or hydroperoxidated FAs) were characterized by LC-MS/MS analyses. Previous investigations suggest that long chain n-3 polyunsaturated FAs (PUFAs) can decrease the risk of mammary carcinogenesis, while the opposite effects were demonstrated by long chain n-6 PUFAs (*44*−*48*). In in vitro studies, the long chain n-3 PUFAs inhibited the growth of both estrogen-dependent and estrogen-independent human breast cancer cell lines (*49*−*57*). Conversely, dietary long chain n-6 PUFAs have been reported to stimulate the growth of human breast cancer cells (*58*, *59*).

In summary, we extracted phytochemicals bound to the RPI and determined the in vitro biological activities in human cancer cell lines and the chemical composition (fingerprint) of the extract. Concentration-dependent antiproliferative effects of the extract and extract-induced apoptosis were detected in all cell lines. This was associated with the induction of proapoptotic bax protein and the cdk inhibitor p21 and the suppression of cdk4 and cyclin D1 activity. We determined the phytochemical fingerprint of RPI by identifying or characterizing 57 phytochemicals by their diagnostic fragmentation patterns and direct comparison with the authentic standards on the basis of ESI-MS/MS data. The major components bound to RPI were FAs, lysoglycerophospholipids, and FA DPHEHP esters. Future studies in our laboratory will further chemically elucidate these phytochemical structures and investigate their bioavailability and bioactivity.

ABBREVIATIONS USED

FITC, fluorescein isothiocyanate; DMSO, dimethyl sulfoxide; MTT, 3-[4,5-dimethylthiazol-2-yl]-2,5-diphenyltetrazolium bromide; SDS−PAGE, sodium dodecyl sulfate−polyacrylamide gel electrophoresis; ER, estrogen receptor; EBV, Epstein−Barr virus; ESI-MS, electrospray ionization mass spectrometry; API, atmospheric pressure interface; ICC, ion charge control; TIC, total ion chromatogram; CID, collision-induced dissociation; lyso-PL, lysophospholipid; lyso-PC, lysophosphatidylcholine; lyso-PE, lysophosphatidylethanolamine; lyso-PG, lysophosphatidylglycerol.

ACKNOWLEDGMENT

We thank Zachary T. Nebus, Don R. McCaskill, and Leo Gingras (Riceland Foods, Inc.) for supplying RPI, Dr. Joshua Epstein for providing the myeloma cell lines, and Drs. R. Terry Pivik and Rosalia C. M. Simmen for helpful comments.

Supporting Information Available: Tables of ESI-MS data for lyso-PCs, lyso-PEs, and lyso-PGs associated with RPI. This material is available free of charge via the Internet at http://pubs.acs.org.

LITERATURE CITED

(1) World Cancer Research Fund and American Institute for Cancer Research, Eds. Patterns of diet and cancer. In *Food, Nutrition and the Prevention of Cancer: A Global Perspective*; American Institute for Cancer Research: Washington, DC, 1997; pp 20−52.

(2) Lamartiniere, C. A.; Murrill, W. B.; Manzolillo, P. A.; Zhang, J. X.; Barnes, S.; Zhang, X.; Wei, H.; Brown, N. M. Genistein alters the ontogeny of mammary gland development and protects against chemically induced mammary cancer in rats. *Proc. Soc. Exp. Biol. Med.* **1998**, *217*, 358−364.

(3) Adlercreutz, H.; Mazur, W. Phyto-oestrogens and Western diseases. *Ann. Med.* **1997**, *29*, 95−120.

(4) Barnes, S.; Sfakianos, J.; Coward, L.; Kirk, M. Soy isoflavonoids and cancer prevention. Underlying biochemical and pharmacological issues. *Adv. Exp. Med. Biol.* **1996**, *401*, 87−100.

(5) Bingham, S. A.; Atkinson, C.; Liggins, J.; Bluck, L.; Coward, A. Phyto-oestrogens: Where are we now? *Br. J. Nutr.* **1998**, *79*, 393−406.

(6) Adlercreutz, C. H.; Goldin, B. R.; Gorbach, S. L.; Hockerstedt, K. A.; Watanabe, S.; Hamalainen, E. K.; Markkanen, M. H.; Makela, T. H.; Wahala, K. T.; Adlercreutz, T. Soybean phytoestrogen intake and cancer risk. *J. Nutr.* **1995**, *125*, 757S−770S.

(7) Arliss, R. M.; Biermann, C. A. Do soy isoflavones lower cholesterol, inhibit atherosclerosis, and play a role in cancer prevention? *Holistic Nursing Pract.* **2002**, *16*, 40−48.

(8) Badger, T. M.; Ronis, J. J.; Simmen, R. C. M.; Simmen, F. A. Soy protein isolate and protection against cancer. *J. Am. Coll. Nutr.* **2005**, *24*, 146S−149S.

(9) Botting, K. J.; Young, M. M.; Pearson, A. E.; Harris, P. J.; Ferguson, L. R. Antimutagens in food plants eaten by Polynesians: Micronutrients, phytochemicals and protection against bacterial mutagenicity of the heterocyclic amine 2-amino-3-methylimidazo[4,5-f]quinoline. *Food Chem. Toxicol.* **1999**, *37*, 95−103.

(10) Kang, M. Y.; Choi, Y. H.; Nam, S. H. Inhibitory mechanism of colored rice bran extract against mutagenicity induced by chemical mutagen mitomycin C. *Agric. Chem. Biotechnol.* **1996**, *39*, 424−429.

(11) Nam, S. H.; Kang, M. Y. *In vitro* inhibitory effect of colored rice bran extracts on carcinogenicity. *Agric. Chem. Biotechnol.* **1997**, *40*, 307−312.

(12) Yasukawa, K.; Akihisa, T.; Kimura, Y.; Tamura, T.; Takido, M. Inhibitory effect of cycloartenol ferulate, a component of rice bran, on tumor promotion in two-stage carcinogenesis in mouse skin. *Biol. Pharm. Bull.* **1998**, *21*, 1072−1076.

(13) Takenaka, S.; Takahashi, K. Enhancement of fecal excretion of poly-chlorinated biphenyls by the addition of rice bran fiber to the diet in rats. *Chemosphere* **1991**, *22*, 375−381.

(14) Aoe, S.; Oda, T.; Tojima, T.; Tanaka, M.; Tatsumi, K.; Mizutani, T. Effects of rice bran hemicellulose on 1,2-dimethylhydrazine-induced intestinal carcinogenesis in Fischer 344 rats. *Nutr. Cancer* **1993**, *20*, 41−49.

(15) Takeshita, M.; Nakamura, S.; Makita, F.; Ohwada, S.; Miyamoto, Y.; Morishita, Y. Antitumor effect of RBS (rice bran saccharide) on ENNG-induced carcinogenesis. *Biotherapy* **1992**, *4*, 139−145.

(16) Hayashi, Y.; Nishikawa, Y.; Mori, H.; Tamura, H.; Matsushita, Y.-I.; Matsui, T. Antitumour activity of (10*E*,12*Z*)-9-hydroxy-10,12-octadecadienoic acid from rice bran. *J. Ferment. Bioeng.* **1998**, *86*, 149−153.

(17) Takeo, S.; Kado, H.; Yamamoto, H.; Kamimura, M.; Watanabe, N.; Uchida, K.; Mori, Y. Studies on an antitumor polysaccharide RBS derived from rice bran. II. Preparation and general properties of RON, an active fraction of RBS. *Chem. Pharm. Bull.* **1988**, *36*, 3609−3613.

(18) Koide, T.; Kamei, H.; Hashimoto, Y.; Kojima, T.; Hasegawa, M. Antitumor effect of hydrolyzed anthocyanin from grape rinds and red rice. *Cancer Biother. Radiopharm.* **1996**, *11*, 273−277.

(19) Akihisa, T.; Yasukawa, K.; Yamaura, M.; Ukiya, M.; Kimura, Y.; Shimizu, N.; Arai, K. Triterpene alcohol and sterol ferulates from rice bran and their antiinflammatory effects. *J. Agric. Food Chem.* **2000**, *48*, 2313−2319.
(20) Guardiola, F.; Codony, R.; Addis, P. B.; Rafecas, M.; Boatella, J. Biological effects of oxysterols: Current status. *Food Chem. Toxicol.* **1996**, *34*, 193−211.
(21) Seetharamaiah, G. S.; Chandrasekhara, N. Studies on hypocholesterolemic activity of rice bran oil. *Atherosclerosis* **1989**, *78*, 219−224.
(22) Sugano, M.; Tsuji, E. Rice bran oil and cholesterol metabolism. *J. Nutr.* **1997**, *127*, 521S−524S.
(23) Nakayama, S.; Manabe, A.; Suzuki, J.; Sakamoto, K.; Inagaki, T. Comparative effects of two forms of gamma-oryzanol in different sterol compositions on hyperlipidemia induced by cholesterol diet in rats. *Jpn. J. Pharmacol.* **1987**, *44*, 135−144.
(24) Morita, T.; Oh-hashi, A.; Takei, K.; Ikai, M.; Kasaoka, S.; Kiriyama, S. Cholesterol-lowering effects of soybean, potato and rice proteins depend on their low methionine contents in rats fed a cholesterol-free purified diet. *J. Nutr.* **1997**, *127*, 470−477.
(25) Ni, W.; Tsuda, Y.; Takashima, S.; Sato, H.; Sato, M.; Imaizumi, K. Anti-atherogenic effect of soya and rice-protein isolate, compared with casein, in apolipoprotein E-deficient mice. *Br. J. Nutr.* **2003**, *90*, 13−20.
(26) Morita, T.; Kiriyama, S. A rice protein isolate alters 7,12-dimethylbenz[*a*]anthracene-induced mammary tumor development in female rats. *J. Nutr. Sci. Vitaminol.* **1996**, *42*, 325−337.
(27) Hakkak, R.; Korourian, S.; Fletcher, T.; Ferguson, M.; Hale, K.; Parker, M.; Holder, D.; Ronis, M. J.; Rowlands, J. C.; Badger, T. M. Lifetime dietary rice protein isolate consumption protects against DMBA-Induced mammary tumors in rats. *Proc. Am. Assoc. Cancer Res.* **2002**, *43*, 823−824.
(28) Morita, T.; Kiriyama, S. Mass production method for rice protein isolate and nutritional evaluation. *J. Food Sci.* **1993**, *58*, 1393−1397.
(29) Fang, N.; Rowlands, J. C.; Casida, J. E. Anomalous structure−activity relationships of 13-homo-13-oxarotenoids and 13-homo-13-oxadehydrorotenoids. *Chem. Res. Toxicol.* **1997**, *10*, 853−858.
(30) Campling, B. G.; Pym, J.; Galbraith, P. R.; Cole, S. P. C. Use of the MTT assay for rapid determination of chemosensitivity of human leukemic blast cells. *Leuk. Res.* **1988**, *12*, 823−831.
(31) Vermes, I.; Haanen, C.; Steffens-Nakken, H.; Reutelingsperger, C. A novel assay for apoptosis: Flow cytometric detection of phosphatidylserine expression on early apoptotic cells using fluorescein labeled Annexin V. *J. Immunol. Methods* **1995**, *184*, 39−51.
(32) Badger, T. M.; Ronis, M. J. J.; Simmen, R. C. M.; Simmen, F. A. Soy protein isolate and protection against cancer. *J. Am. Coll. Nutr.* **2005**, *24*, 146S−149S.
(33) Morgan, D. O. Principles of CDK regulation. *Nature* **1995**, *374*, 131−134.
(34) Fang, N.; Yu, S.; Badger, T. M. LC-MS/MS analysis of lysophospholipids associated with soy protein isolate. *J. Agric. Food Chem.* **2003**, *51*, 6676−6682.
(35) Rentel, C.; Strohschein, S.; Albert, K.; Bayer E. Silver-plated vitamins: A method of detecting tocopherols and carotenoids in LC/ESI-MS coupling. *Anal. Chem.* **1998**, *70*, 4394−4400.
(36) Marinetti, G. V.; Cattieu, K. Composition of phospholipids of human leukocytes. *Chem. Phys. Lipids* **1982**, *31*, 169−177.
(37) Portman, O. W.; Alexander, M. Lysophosphatidylcholine concentrations and metabolism in aortic intima plus inner media: Effect of nutritionally induced atherosclerosis. *J. Lipid Res.* **1969**, *10*, 158−165.
(38) Schiller, J.; Zschörnig, O.; Petkoviæ, M.; Müller, M.; Arnhold, J.; Arnold, K. Lipid analysis of human HDL and LDL by MALDI-TOF mass spectrometry and ^{31}P NMR. *J. Lipid Res.* **2001**, *42*, 1501−1508.
(39) Croset, M.; Brossard, N.; Polette, A.; Lagarde, M. Characterization of plasma unsaturated lysophosphatidylcholines in human and rat. *Biochem. J.* **2000**, *345*, 61−67.
(40) Huang, M.; Graeler, M.; Shankar, G.; Spencer, J.; Goetzl, E. Lysophospholipid mediators of immunity and neoplasia. *Biochim. Biophys. Acta* **2002**, *1582*, 161−167.
(41) Tigyi, G. Lysolipid mediators in cell signaling & disease. *Biochim. Biophys. Acta* **2002**, *1582*, VII.
(42) Gräler, M. H.; Goetzl, E. Lysophospholipids and their G protein-coupled receptors in inflammation and immunity. *Biochim. Biophys. Acta* **2002**, *1582*, 168−174.
(43) Sugiyama, S.; Kugiyama, K.; Ogata, N.; Doi, H.; Ota, Y.; Ohgushi, M.; Matsumura, T.; Oka, H.; Yasue, H. Biphasic regulation of transcription factor nuclear factor-*K*B activity in human endothelial cells by lysophosphatidylcholine through protein kinase C-mediated pathway. *Arterioscler. Thromb. Vasc. Biol.* **1998**, *18*, 568−576.
(44) Maillard, V.; Bougnoux, P.; Ferrari, P.; Jourdan, M. L.; Pinault, M.; Lavillonniere, F. N-3 and N-6 fatty acids in breast adipose tissue and relative risk of breast cancer in a case-control study in Tours, France. *Int. J. Cancer* **2002**, *98*, 78−83.
(45) Mukutmoni-Norris, M.; Hubbard, N. E.; Erickson, K. L. Modulation of murine mammary tumor vasculature by dietary n-3 fatty acids in fish oil. *Cancer Lett.* **2000**, *150*, 101−109.
(46) Liu, X. H.; Rose, D. P. Suppression of type IV collagenase in MDA-MB-435 human breast cancer cells by eicosapentaenoic acid in vitro and in vivo. *Cancer Lett.* **1995**, *92*, 21−26.
(47) Rose, D. P.; Connolly, J. M. Effects of dietary omega-3 fatty acids on human breast cancer growth and metastases in nude mice. *J. Natl. Cancer Inst.* **1993**, *85*, 1743−1747.
(48) Rose, D. P.; Connolly, J. M.; Rayburn, J.; Coleman, M. Influence of diets containing eicosapentaenoic or docosahexaenoic acid on growth and metastasis of breast cancer cells in nude mice. *J. Natl. Cancer Inst.* **1995**, *87*, 587−592.
(49) Chajs, V.; Sattler, W.; Stranzl, A.; Kostner, G. M. Influence of n-3 fatty acids on the growth of human breast cancer cells in vitro: Relationship to peroxides and vitamin E. *Breast Cancer Res. Treat.* **1995**, *34*, 199−212.
(50) Chamras, H.; Ardashian, A.; Heber, D.; Glaspy, J. A. Fatty acid modulation of MCF-7 human breast cancer cell proliferation, apoptosis and differentiation. *J. Nutr. Biochem.* **2002**, *13*, 711−716.
(51) Grammatikos, S. I.; Subbaiah, P. V.; Victor, T. A.; Miller, W. M. N-3 and N-6 fatty acid processing and growth effects in neoplastic and noncancerous human mammary epithelial cell lines. *Br. J. Cancer* **1994**, *70*, 219−227.
(52) Germain, E.; Chajes, V.; Cognault, S.; Lhuillery, C.; Bougnoux, P. Enhancement of doxorubicin cytotoxicity by polyunsaturated fatty acids in the human breast tumor cell line MDA-MB-231: Relationship to lipid peroxidation. *Int. J. Cancer* **1998**, *75*, 578−583.
(53) Kachhap, S. K.; Dange, P. P.; Santani, R. H.; Sawant, S. S.; Ghosh, S. N. Effect of omega-3 fatty acid (docosahexanoic acid) on BRCA1 gene expression and growth in MCF-7 cell line. *Cancer Biother. Radiopharm.* **2001**, *16*, 257−263.
(54) Noguchi, M.; Earashi, M.; Minami, M.; Konoshita, K.; Miyazaki, I. Effects of eicosapentaenoic and docosahexaenoic acid on cell growth and prostaglandin E and leukotriene B production by a human breast cancer cell line (MDA-MB-231). *Oncology* **1995**, *52*, 458−464.
(55) Rose, D. P.; Connolly, J. M. Effects of fatty acids and inhibitors of eicosanoid synthesis on the growth of a human breast cancer cell line in culture. *Cancer Res.* **1990**, *50*, 7139−7144.
(56) Wang, M.; Liu, Y. E.; Ni, J.; Aygun, B.; Goldberg, I. D.; Shi, Y. E. Induction of mammary differentiation by mammary-derived growth inhibitor-related gene that interacts with an omega-3 fatty acid on growth inhibition of breast cancer cells. *Cancer Res.* **2000**, *60*, 6482−6487.

(57) Yamamoto, D.; Kiyozuka, Y.; Adachi, Y.; Takada, H.; Hioki, K.; Tsubura, A. Synergistic action of apoptosis induced by eicosapentaenoic acid and TNP-470 on human breast cancer cells. *Breast Cancer Res. Treat.* **1999**, *55*, 149−160.

(58) Kachhap, S. K.; Dange, P.; Nath Ghosh, S. Effect of omega-6 polyunsaturated fatty acid (linoleic acid) on BRCA1 gene expression in MCF-7 cell line. *Cancer Lett.* **2000**, *154*, 115−120.

(59) Razanamahefa, L.; Prouff, S.; Bardon, S. Stimulatory effect of arachidonic acid on T-47D human breast cancer cell growth is associated with enhancement of cyclin D1 mRNA expression. *Nutr. Cancer* **2000**, *38*, 274−280.

Received for review February 28, 2006. Revised manuscript received April 19, 2006. Accepted April 19, 2006.

JF0605852